Eleventh Southeast Asian Geotechnical Conference, 4-8 May, 1993, Singapore

Review of Miniature Soil Probes For Model Tests

M D BOLTON Cambridge University, United Kingdom
M W GUI Cambridge University, United Kingdom
R PHILLIPS Cambridge University, United Kingdom

SYNOPSIS : The use of miniature vane and CPT probes in centrifuge models is reviewed. Some data of tests in sands and clays is presented. It is shown to be essential to perform soil tests in flight; otherwise the swelling which follows the cessation of centrifuging would lead to softening. Methods of normalisation are suggested for vane and cone data. Dimensional analysis and modelling of models is used to demonstrate the importance of distinguishing shallow and deep penetration mechanisms for cones which are large relative to stratum depth. Soil particle size is shown to be insignificant if less than one twentieth the cone diameter. The effects of stress level, particle crushing, OCR, and proximity of boundaries are also mentioned.

1 INTRODUCTION

Centrifuges have been widely adopted in modelling geotechnical problems because, without the expense and delay of doing full-scale tests, the behaviour of a foundation can be observed in a soil specimen of known parameters. Perhaps the most important feature of centrifuge tests is the simulation of self-weight to replicate full scale stresses.

Parameters are effective stress level dependent. Hence, in order to determine soil parameters relevant to models, in-flight tests must be carried out. Probes scaled down according to the modelling scale factor would be impossibly small. On the other hand, full size probes would be too big in relation to model size. Hence miniature probes are preferred but scale distortions must be accounted for.

This paper discusses some observations encountered when using miniature vane shear and cone penetrometer apparatus in centrifuge tests. Some results are presented for clay and sand. The correlations for these in-flight strength tests are also reported.

2 VANE SHEAR TEST IN CLAY

The details and operation of the vane shear apparatus, Fig 1, were described by Almeida (1984). The rotation of the shaft is measured by a rotary potentiometer (F), while the depth of penetration is measured by an displacement transducer (A). Two DC motors (D & E), are used to advance the shaft into the soil and rotate the blades. The total shaft friction and shear resistance of the vane are monitored by a torque cell (G), on the shaft. The shaft friction can be estimated separately, Fig 2, during a delay in vane rotation caused by a slip coupling at the connection of the shear vane and the shaft. Failure to account for shaft friction causes a false indication of strength increasing

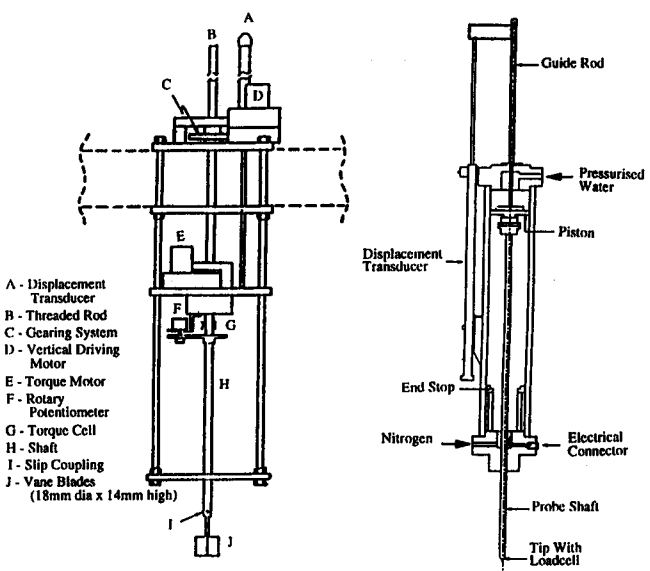

Fig.1 Miniature Vane Shear & Cone Penetrometer Apparatus

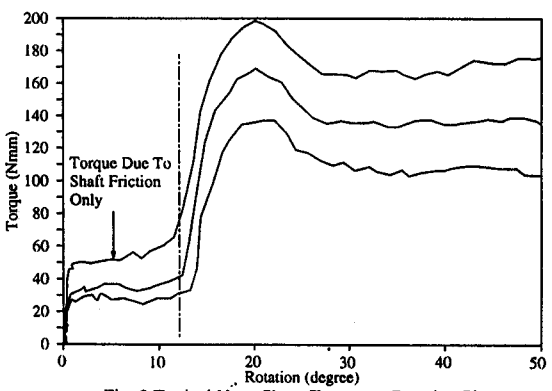

Fig. 2 Typical Vane Shear Torque vs Rotation Plots

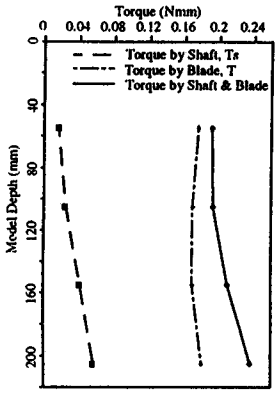

Fig. 3 Measurement With Vane Mark II (after Almeida, 1984)

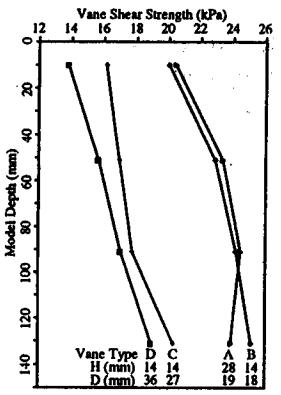

Fig. 4 Influence of Vane Geometry (after Cheah, 1981)

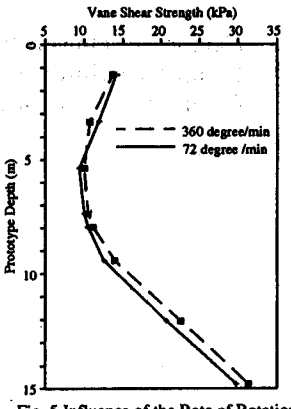

Fig. 5 Influence of the Rate of Rotation (after Almeida, 1984)

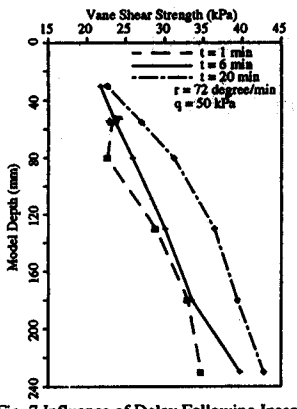

Fig. 7 Influence of Delay Following Insertion (after Almeida, 1984)

with depth. Fig 3 shows the torque due to the blade almost constant with depth while torque due to shaft friction increases with depth. The test was carried out at 1g in a large clay consolidometer.

2.1 Factors Influencing Vane Shear Strength

1. Vane Geometry

On back-analysis, it is assumed that a solid cylinder of clay is forced to rotate relative to the parent body, and that the same peak strength is mobilised on both vertical and horizontal surfaces at peak torque. Fig 4 showed that there was a 30% decrease in apparent undrained shear strength if the H/D ratio of the vane head was reduced from 1.5 to 0.4. This is far higher than could be accounted for by anisotropy, and must indicate that the mechanism of failure is no longer a simple cylinder when H/D < 0.8. No significant changes in indicated strength were found for H/D > 0.8.

2. Rate of Rotation

Blight (1968) suggested a time factor, T_v, for an undrained condition (degree of drainage less than 10%) to be :

$$T_v = c_v t_f / D < 0.02 \text{ to } 0.04 \qquad ..(1)$$

where c_v is the coefficient of consolidation and t_f is the time to failure. Further study by Matsui and Abe (1981) also suggested that the undrained condition for kaolin can be achieved if the rate of rotation is greater than 60o/min. This rate of rotation would also satisfy undrained behaviour in more typical clays which would be less permeable than kaolin. The effect of even faster rates of rotation of the vane in clay was investigated and found to be not very significant. An increase in the rate of rotation from 72°/min to 360°/min resulted in a variation in shear strength of about 6% to 10%, Fig 5. The time factor for this rate of rotation is about Tv=0.035 which is within the recommended range.

3. Water Entry

Water entry from the clay surface to the vane head, passing down from the cruciform wound left by the blades, can cause the undrained shear strength to be underestimated due to local swelling and softening. Fig 6 shows a vane test

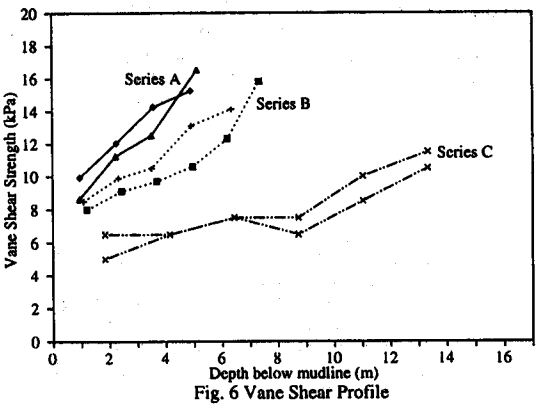

Fig. 6 Vane Shear Profile

series A conducted without surface water entry, a series B in which water entry was not prevented, and a series C in which tests were conducted with a hand vane immediately after the centrifuge was stopped. Water entry was prevented in series A by pushing the shear vane through a clay mound which was proud of the surrounding submerged clay surface. Series C results show the inaccuracy which may occur in post-flight measurements.

4. Delay Following Insertion

The influence of the delay between vane insertion and the start of the rotation are shown in Fig 7. These tests were carried out in a consolidometer. As the delay increases, the strength of soft clay increases due to the dissipation of excess pore pressures set up during vane insertion.

2.2 Analysis of Vane Results

The undrained shear strength, c_u, is assessed from the peak torque, T, mobilised by vane blade alone. It was assumed that the behaviour around the vane blade is undrained and that a constant shear strength is mobilised around the cylindrical surface exscribed by the blade, thus;

$$T = c_u(3H+D)\pi D^2/6 \qquad ..(2)$$

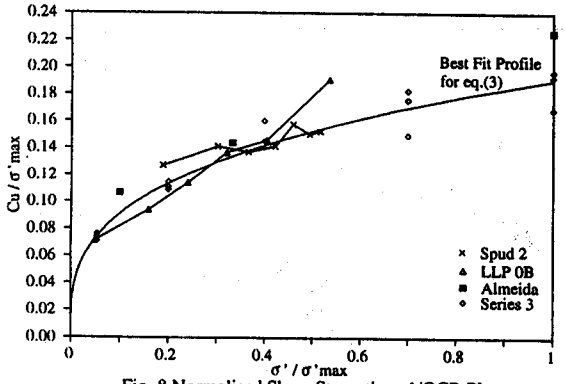

Fig. 8 Normalised Shear Strength vs 1/OCR Plot

Undrained shear strength is defined in terms of undrained behaviour but it is also dependent on stress history (Terzaghi, 1936), sample orientation, initial effective stress states and stress paths to failure. Schofield & Wroth (1968) proposed a relationship between c_u, σ_v', and OCR, in the form;

$$c_u = \sigma_v' (a * OCR^b) \qquad ..(3)$$

The normalised peak shear strength from several laboratory and centrifuge tests are plotted against normalised effective vertical stress in Fig 8. For kaolin clay, values of a=0.19 and b=0.67 have been proposed for equation (3), Hamilton et al (1991).

3 CPT IN CLAY

Cone penetration tests (CPT) can be carried out more quickly than vane tests and produce a full profile of the soil resistance. However, in order to obtain the strength of clay, it is necessary to calibrate the tip resistance against shear strength. The probe has a tip with a 60° apex and a load cell is mounted immediately after the tip, Fig 1.

3.1 Factors Influencing Tip Resistance In Clay

1. Penetration Rate

Fig 9 compares the resistance profiles for tests carried out at different penetration rates. Test MWG2-T1 was the first to be carried out on the clay sample after it had reached equilibrium.

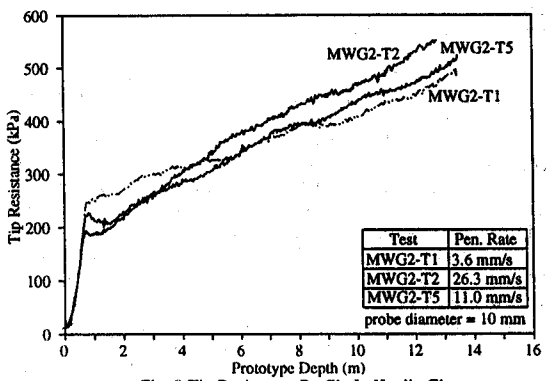

Fig. 9 Tip Resistance Profile In Kaolin Clay

Other tests were done following an unloading-reloading cycle, due to the necessity to stop the centrifuge and move the probe into a fresh location. There is some scatter, but the increase in tip resistance for a test done at 26.3mm/s was never more than 13% compared to a test done at 11mm/s.

2. Pore Pressure at Shoulder

Baligh et al (1981) and Campanella & Robertson (1981) have pointed out this problem in all existing designs of cone. For a miniature probe, the actual pore pressure distribution around the shoulder is unknown. However, the effect is only significant when interpreting CPT data in soft clays where the excess pore pressures are large in relation to tip resistance, (Crooks & Been, 1988).

3.2 Analysis of CPT Results in Clay

In order to evaluate the shear strength of clay, tip resistance has to be converted into cone factor, N_c, which can be assessed by assuming;

$$q_c = \sigma_v + N_c c_u \qquad ..(4)$$

where c_u can be assessed from equation (3). A plot of some tests in soft kaolin clay is presented in Fig 10. The rather low values for deep penetrations (9 instead of the usually assumed 10-12) may be due to the lack of pore pressure correction, as explained above.

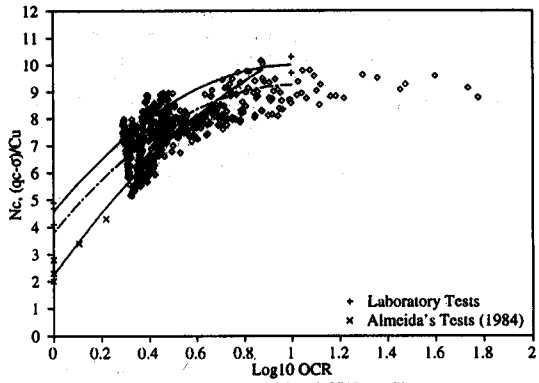

Fig. 10 Analysis of CPT on Clay

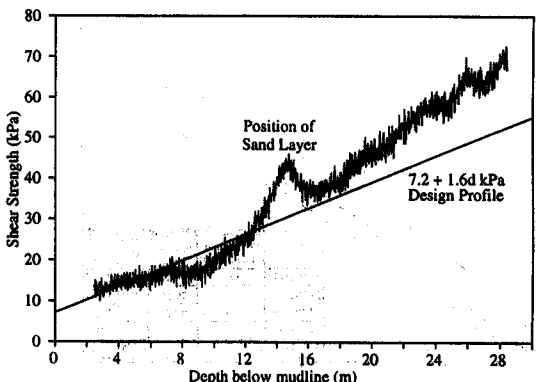

Fig. 11 Shear Strength Profile Derived From CPT

By adopting the best fitted N_c profile from these tests, the shear strength profile for a clay can be determined, Fig 11. The profile compares reasonably well with the preferred profile until the level of the intermediate sand layer; thereafter, the shear strength is higher. This is probably caused by the sand layer (and filter paper) which is restraining the failure mechanism around the cone penetrometer.

4 CPT IN SAND

4.1 Factors Influencing Tip Resistance In Sand

An analysis of CPTs in sand reveals the following function of dimensionless groups:

$$\frac{(q_c - \sigma_v)}{\sigma_v'} = N_p\left(\phi_{crit}, \frac{\sigma_v'}{p_c}, OCR, I_D, \frac{z}{B}, \frac{B}{d}\right) \quad ..(5)$$

where ϕ_{crit} and p_c refer to intrinsic soil properties (angle of shearing resistance at constant volume, and an aggregate crushing parameter defined in Bolton, 1986); σ_v', OCR and I_D refer to the current soil state (the initial effective vertical stress, overconsolidation ratio which affects earth pressure coefficient, and relative density); z/B and B/d describe test geometry (test depth to cone diameter ratio, and cone to particle diameter ratio). Some care has to be taken to isolate the effect of each term on the dimensionless penetration coefficient N_p.

1. Overconsolidation Effect

Overconsolidation is easy to investigate in the centrifuge, tests being repeated in identical circumstances at identical accelerations n, the soil having been previously raised to different maximum accelerations OCRn. Lee (1990) observed an overconsolidation effect in dense 25/52 Leighton Buzzard (LB) sand, and his result, in Fig 12, correlated well with Schmertmann's (1975) empirical formula

$$q_{c(oc)} = q_{c(nc)}[1+\alpha(OCR^{\beta} - 1)] \quad ..(6)$$

where α=0.75 and β=0.42.

However, there was no appreciable difference in the tip resistance profile for test MWG1-T5 in the finer and more rounded Fontainbleau sand (FB) which was conducted at an OCR of 1.95.

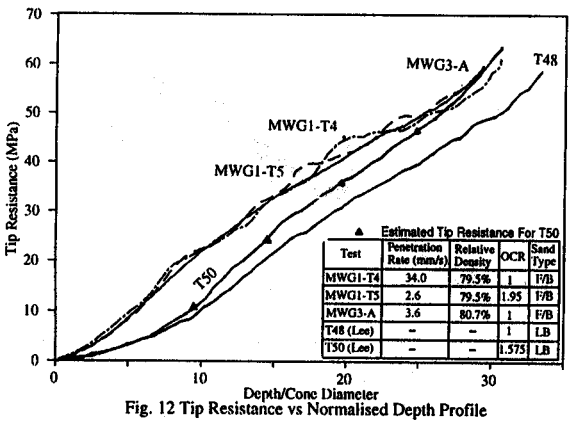

Fig. 12 Tip Resistance vs Normalised Depth Profile

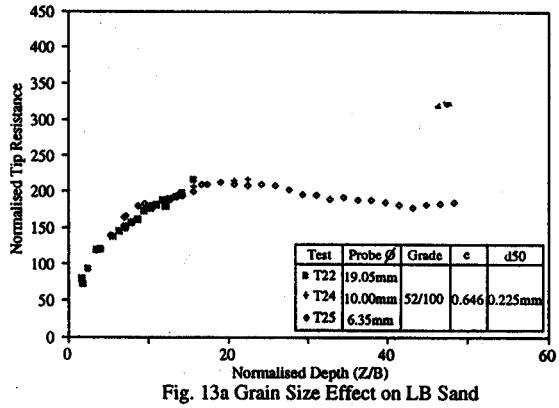

Fig. 13a Grain Size Effect on LB Sand

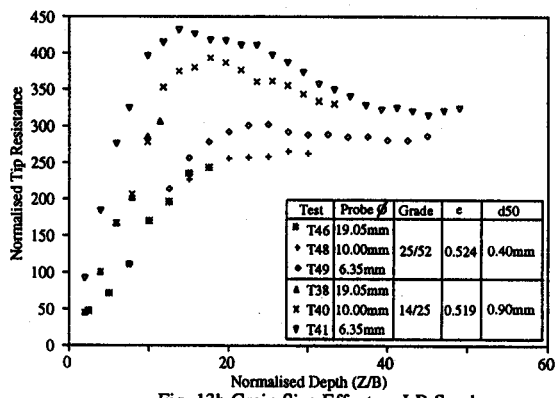

Fig. 13b Grain Size Effect on LB Sand

2. Geometry Effect

The effect of probe geometry on the coefficient N_p can best be shown in Fig 13a for fine LB sand at a single relative density, where N_p is plotted against depth ratio z/B for cones of different diameter. It is necessary to preserve constant stress level σ_v' at each z/B, so as to keep the ratio σ_v'/p_c (in equation 5) constant for the different cones. Now $\sigma_v' = \rho z.ng$ which can be written $\rho(z/B)g.nB$ so it was necessary to keep nB constant. Each test therefore modelled a single prototype cone, of 0.4m diameter in this case. Fig 13a shows that the data from this modelling-of-models trial nicely superimposes until each cone approaches the base of the test container. This proves that the soil particle size does not affect the result for ratio B/d in the range 85 to 28.

Fig 13b repeats the same plot for medium and coarse LB sand. Treating each soil separately, the plots for the medium sand merge reasonably well for B/d = 48 and 25, but there is a suggestion of a small amount of extra resistance at B/d = 16. For the coarse sand, all the data are somewhat higher and while there is insufficient evidence of distortion in reducing B/d from 21 to 11, it can be seen that a further reduction to 7 does raise resistance especially at shallow depth. Some extra resistance, presumably due to the loss of degrees of freedom, must therefore be anticipated if the cone/particle diameter ratio is permitted to fall below about 20.

In each case, however, it is clear that there are two phases of behaviour depending on the depth ratio z/B. Shallower than some critical ratio (z/B ≈ 20 in Fig 13) the coefficient increases with depth ratio in the fashion of shallow foundations. Below this critical depth, the coefficient seems to hold steady, or to fall slightly, characteristic of deep foundations. The dichotomy was observed by Meyerhof (1983) in his 1g tests on model piles. This geometrical effect is highly significant in model tests with probes which are large relative to the depth of strata, whereas it would be insignificant in the field. New CPT correlations will be required, appropriate to shallow probes.

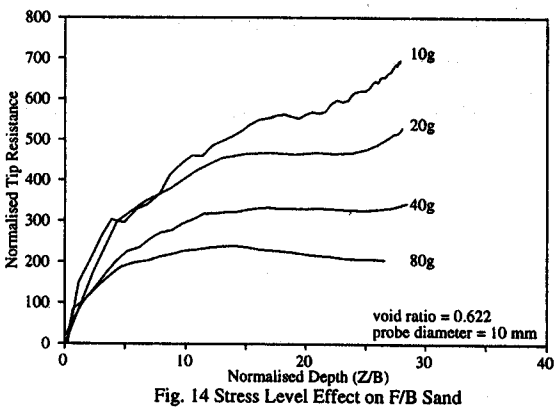

Fig. 14 Stress Level Effect on F/B Sand

3. Stress Effect

Differently sized soil grains may have different p_c values, and the consequential difference in σ_v'/p_c may explain part of the variance between curves for the three grades of sand in Fig 13. In addition, different degrees of angularity confer different values of ϕ_{crit}. Furthermore, the relative density of the medium and coarse soils in Fig 13b was $I_D \approx 0.92$, whereas that of the fine soil in 13a was about 0.82.

The most reliable way to investigate stress effects is to plot N_p against z/B holding B/d constant, for a particular soil at a particular density, but to test at different acceleration ratios n so that only σ_v'/p_c varies. Fig 14 shows that as stresses rise, the values of N_p fall, presumably due to the enhanced tendency for crushing to suppress dilatancy. It is clearly necessary to account separately for crushing and relative density, as already demonstrated in the correlations of Jamiolkowski et al (1985) for deep probes.

4. Boundary Effect

Phillips and Valsangkar (1987) carried out CPT in FB sand (I_D=87%) in a rigid-wall tub. Fig 15 shows the results of the tests done using a 10mm probe at a distance of 10B, 20B and 42B from the rigid-wall. No boundary effect was observed. However, Lee (1990) concluded that the basal boundary effect could be significant, especially for dense sands at small stress levels as shown already in Fig 14.

5. Penetration Rate Effect

There is no apparent penetration rate effect in the range of 3.6 to 34mm/s for test carried out

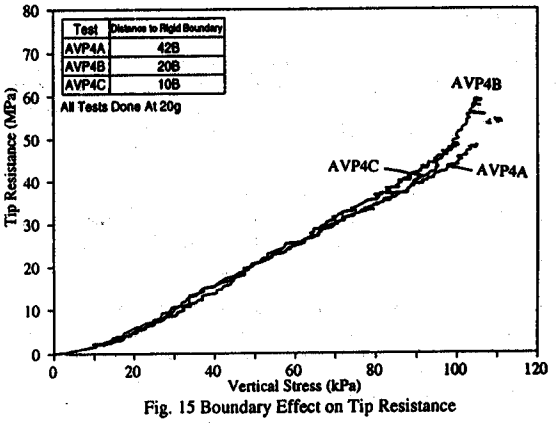

Fig. 15 Boundary Effect on Tip Resistance

in FB sand, Fig 12. Lee (1990) also concluded that the penetration rate in the range of 3.5 to 27mm/s for test done in 14/25 and 52/100 LB sand is insignificant.

4.2 Analysis of CPT Results in Sand

Bolton (1986) proposed to consider the mobilized angle of friction as a function of initial relative density, critical angle of internal friction and mean effective stress. Since the tip resistance is dependent on the relative density and mean effective stress, his empirical correlation can be used to predict the internal angle of friction of the sand tested. For triaxial tests,

$$\phi'_{max}-\phi'_{crit} = 3I_R \quad (\text{For } 0 < I_R < 4) \quad ..(7)$$

$$I_R = I_D[10-\ln(p')] - 1 \quad ..(8)$$

where p' is the mean effective stress and I_R is defined as a relative dilatancy index. For CPT, it was assumed that the mean effective stress is equal to the geometric mean of the probe resistance and the vertical effective stress;

$$p' = \sqrt{(\sigma_v' q_c)} \quad ..(9)$$

To calculate ϕ'_{max}, it was assumed that ϕ'_{crit} for FB sand is 32° and the results are plotted in Fig 16. The curve seem to correlate well with the low pressure triaxial data.

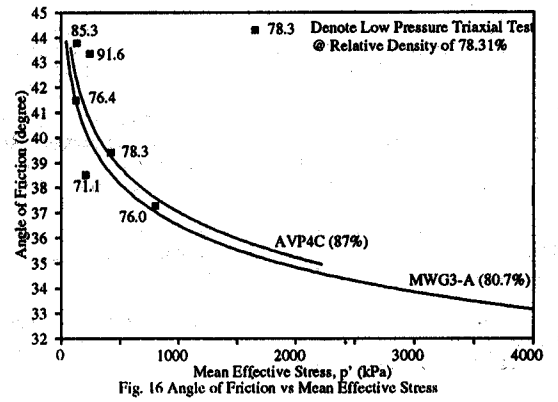

Fig. 16 Angle of Friction vs Mean Effective Stress

5 CONCLUSIONS

The observations and the analysis of the results of 2 miniature probes for assessing consistency of sample preparation and strength characteristics of soils for centrifuge tests is presented.

It has been shown that tests on clay must be performed in flight to avoid post-test swelling, and that water entry prior to testing must be minimised.

Cone tests in sand produce unbiased results if the cone/particle size ratio exceeds 20, but account must be taken of the different resistances of shallow and deep probes, defined in relation to depth/diameter ratio.

Work is currently being carried out in several European centrifuge centres, with the aim to recommend a standard procedure and analysis for CPTs in sand and clay samples.

REFERENCES

Almeida, M.S.S. (1984). Stage constructed embankments on soft clay. PhD Thesis, Cambridge University.

Baligh, M.M., Assouz, A.M., Wissa, A.Z.E., Martim, R.T. and Morrisson, M.J. (1981). The piezocone penetrometer. Proc. Conf. On Cone Penetration Testing and Experience, St.Louis, Missouri.

Blight, G.E. (1968). A note on field vane testing of silty soils. J. Canadian Geotech. v5, No 3, 142-149.

Bolton, M.D.(1986). The strength and dilatancy of sands. Geotechnique 36, No 1, 65-78.

Campanella, R.G. and Robertson, P.K. (1981). Applied cone research. Proc. Cone Penetration Testing And Experience, St.Louis, Missouri, 343-362.

Cheah, H. (1981). Site investigation techniques for laboratory soils models. M.Phil. Thesis, Cambridge University.

Crooks, J.H.A. and Been, K. (1988). CPT interpretation in clay. Proc. 1st ISOPT, Orlando, 715-722.

Hamilton, J.M., Phillips, R., Dunnavant, T.W. and Murff, J.D. (1991). Centrifuge study of laterally loaded pile behaviour in clay. Int. Conf. Centrifuge'91, Boulder, 285-294.

Jamiolkowski, M., Ladd, C.C., Germaine, J.T. and Lancellota, R. (1985). New developments in field and laboratory testing of soils, Proc. 11th ICSMFE, San Francisco, v1, 57-153.

Lee, S.Y. (1990). Centrifuge modelling of cone penetration testing in cohesionless soils. PhD Thesis, Cambridge University.

Matsui, T. and Abe, N. (1981). Shear mechanism of vane test in soft clays. Soils and Foundations 21, No 4, 69-80.

Meherhof, G.G. (1983). Scale effects of ultimate pile capacity. ASCE J. Geotech. Eng. Div., v109, GT6, 797-806.

Phillips, R. and Valsangkar, A.J. (1987). An experimental investigation of factors affecting penetration resistance in granular soils in centrifuge modelling. Tech. Report, Cambridge University : CUED/D-Soils/TR210.

Schmertmann, J.H. (1975). Measurement of in-situ shear strength. Proc. Conf. on In-situ Measurement of Soil Properties. Raleigh (N. Carolina), 57-138.

Schofield, A.N. and Wroth, C.P. (1968). Critical State Soil Mechanics, McGraw Hill.

Terzaghi, K. (1936). The shearing resistance of saturated soils and the angle between the planes of shear, Proc. 1st ICSMFE, v1, 54-56.